

APPLICATION OF LIF-TECHNIQUE TO ATMOSPHERIC PRESSURE PLASMAS

T.Oda and R.Ono

School of Engineering, the University of Tokyo, 7-3-1 Hongo, Bunkyo-ku, Tokyo 113-8656, Japan

1 Introduction

The atmospheric pressure **non-thermal plasma** has been extensively studied for decomposing environmental pollutants such as SO_x [1], NO_x [2,3], and VOCs [4,5] (volatile organic compounds). Many researchers have been engaged in developing removal technique of those toxic pollutants with the non-thermal plasma. A high energy electron beam (EB) irradiation is also very effective to remove SO_x, NO_x in the combustion flue gas or various toxic VOCs in the air [6,7]. All flue gas from 220MW heavy oil power station at Nagoya is tested by that EB process. Discharge plasma is generated by various kinds of modes. The barrier discharge and the surface discharge can generate the non-thermal plasma easily by commercial frequency or high frequency (kHz order) high voltage at atmospheric pressure. The DC corona discharge can produce the non-thermal plasma with poor energy efficiency. The RF or millimeter wave plasma is medium state from the non-thermal plasma to the thermal plasma. The thermal plasma was also tested to decompose high density fluorocarbon (CFC)[8]. A submicrosecond pulse corona can decompose NO_x and dioxin in the flue gas. A packed-bed reactor was also studied with a little bit poor energy efficiency but with low emission of ozone. For practical usage of the non-thermal plasma as toxic gas removal technique, the improvement of the energy efficiency and preventing the production of hazardous byproducts are very essential. Recent good result is that the input discharge power of 20 J/l can decompose more than 90 % trichloroethylene (TCE) in air where TCE concentration is 100 or 1,000 ppm with the aid of the catalyst inserted in the plasma region [9]. To improve the energy efficiency, chemical reactions in the plasma must be clear but most reactions and parameters are still under the research. Computational analysis of those mechanisms has been done by some researchers [10,11]. Some parameters were observed experimentally [12]. They predicted reaction channels of gas removal and regarded some radicals as principal species in the reaction channels. Identification of those radicals (and molecules/atoms) in the plasma is necessary to analyze reaction channels and to determine the reaction rate. However, still only a few researches on direct observation of those radicals in the atmospheric pressure plasma because of the technological difficulties. Laser-Induced Fluorescence (LIF) technique is developed for those radical analysis. LIF is used for the radical analysis of the low pressure (low temperature plasma) in the semiconductor process [13~15], steady state combustion flame analysis[16~19] or atmospheric chemistry[20]. Recently, some researchers tried to introduce that LIF technique as the atmospheric pressure plasma diagnosis observing time and spatial distribution analysis of those radicals. Those discharge plasma is nanoseconds pulse and non-equilibrium conditions which cause difficulties of LIF application. The target radicals of those LIF experiments include N [16], O [13, 17, 20], OH [17, 18] and NO_x [17, 19]. Recently the authors succeeded to observe two-dimensional distribution of OH radicals in various kinds of pulse discharge plasmas, such as equilibrium [21] or non-thermal plasma [22] as time variation. Other Japanese international group also observed NO distribution during DC corona [23] or ultra short pulse corona [24] in Japan. The authors also observed similar NO removal pattern by LIF. This paper introduces those radical distributions related with discharge plasmas for better understanding of plasma chemical reactions in Japan.

2 Laser Induced Fluorescence (LIF) technique

2.1 Principle of LIF

Laser Induced Fluorescence (LIF) method is one of laser spectroscopy techniques to measure the density and temperature of molecules, atoms, radicals and others. LIF technique needs a frequency-tunable laser with a narrow spectral line width to excite electrons from one level to upper level. The principle of LIF can be explained by a 3-state model shown in Fig.1. The model represents simplified energy-levels of a molecule.

In the case of measuring the number density of molecules in the state 1, the lowest level in Fig.1, the laser wavelength was set to excite a $1 \rightarrow 2$ transition. The molecules absorb the laser light (photon) and ground level electron (in the state 1) is excited to the state 2 with a rate of $B_{12}I_L$. Then the excited electrons in the molecules relax to lower states with spontaneous emission of light with a rate of A_{2i} , with stimulated emission with a rate of $B_{2i}I_L$, and with quenching caused by collisions with surrounding molecules with a rate of Q_{2i} .

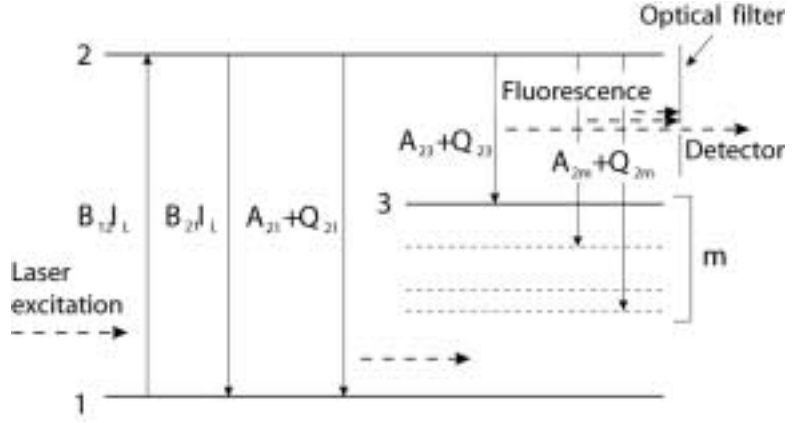


Fig.1 A simplified 3-state model. $1 \rightarrow 2$: excitation transition; $2 \rightarrow 3$: fluorescence transition; A_{ij} , B_{ij} : Einstein coefficients of $i \rightarrow j$ transition; Q_{ij} : quenching rate of $i \rightarrow j$ transition; I_L : laser power density.

The emission from a $2 \rightarrow 3$ transition is detected through an optical bandpath filter which eliminates stray light and background emission. The LIF signal intensity I_{LIF} , defined as the intensity of the $2 \rightarrow 3$ emission, is proportional to the number density of the state 1 N_1 . It is derived from rate equations

$$\frac{d}{dt} N_1 = A_{21}N_2 - B_{12}I_L(N_1 - N_2) \quad (1)$$

$$\frac{d}{dt} N_2 = -(Q_2 + A_{21})N_2 + B_{12}I_L(N_1 - N_2) \quad (1')$$

where $A_2 = \sum_i^m A_{2i}$ $Q_2 = \sum_i^m Q_{2i}$ and the definition of I_{LIF} is

$$I_{LIF} = V \int_0^{\tau_L} A_{23}N_2(t)dt \quad (2)$$

where V is the volume of molecules and τ_L is the pulse width of the incident laser. Assuming that $B_{12}I_L\tau_L \ll 1$, the following equations can be obtained from Eqs.(1) and (2)

$$I_{LIF} = V \frac{A_{23}}{Z_2} B_{12}I_L\tau_L N_1 \quad (Z_2 \gg B_{12}I_L) \quad (3)$$

$$V A_{23} \tau_L N_1 \quad (Z_2 \ll B_{12}I_L) \quad (3')$$

where

$$Z_2 = Q_2 + A_2. \quad (4)$$

2.2 Determination of temperature

The temperature of the molecules can be determined by measuring the several numbers of density of states. The distribution of those numbers is defined as the following equation at temperature of T ,

$$N_i \propto g_i \exp\left(-\frac{E_i}{kT}\right) \quad (5)$$

where g_i and E_i are degeneracy and energy of level i , respectively. The plot of N_i in arbitrary unit versus E_i gives the temperature T .

2.3 Other spectroscopic techniques

There are some other spectroscopic techniques which may be used as a diagnosis of the atmospheric pressure non-thermal plasma. In this section, those techniques are briefly described comparing with LIF.

2.3.1 Optical emission spectroscopy(OES)

Optical emission spectroscopy in the discharge plasma is the most major spectroscopic method. This method detects spontaneous emission from excited molecules where excitation is due to the plasma or some chemical reactions. As that experiment does not need an expensive tuner laser for exciting molecules, it is easy to observe OES only with the monochromator and the photo-detector. The disadvantage of this method is that it can not observe molecules in the ground state whose density is an important factor in many cases.

2.3.2 Absorption spectroscopy

LIF requires two steps, (1) exciting specific molecules (or radicals) by laser absorption and (2) detecting fluorescence from those excited molecules. The absorption spectroscopy requires only the step (1). When the laser whose wavelength is adjusted to excite those specific molecules irradiates research area, those molecules absorb light and input power, I_0 , reduces to I_l . The density of the target molecules can be determined from the ratio of I_l/I_0 . The observed density by that is accurate because of the no quenching effect. Monochromatic light source can be used but the disadvantage of that method is that (1) the sensitivity is low (SN ratio), and (2) measurement of two-dimensional density profile is very difficult.

2.3.3 CARS

CARS (coherent anti-stokes Raman spectroscopy) uses two lasers whose wavelength are ν_0 and ν_p , respectively. CARS requires that $\nu_0 - \nu_p$ which is resonant with specific molecules. Irradiation of two laser beams to the measurement area yields scattered light ($\nu_A = \nu_0 + (\nu_0 - \nu_p)$) whose intensity is determined by the density of the specific molecules. As the CARS signal radiates like a beam, the background light can be greatly reduced. The disadvantage of this method is that (1) the sensitivity is low, and (2) the system is very complex because it needs two lasers.

3 OH-LIF

3.1 OH excitation

For OH radical observation by LIF technology, two different laser sources are used. The first one is a dye laser whose oscillating frequency is doubled by a second harmonics generator. That dye laser excites the A - X(1,0) band of OH radicals at 282 nm. Another laser is a tunable KrF excimer laser which excites the A - X(3,0) band at 248 nm. For atmospheric pressure plasma diagnosis, the second KrF laser excitation is more desirable than the first one because of low quenching effect, which is described in the next section.

3.2 Quenching

LIF measurement has a large problem caused by quenching at high pressure, for example, atmospheric pressure.

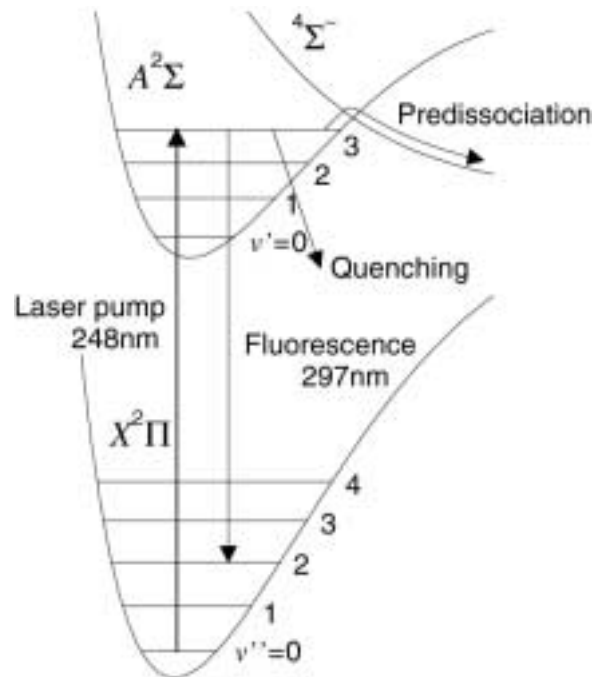


Fig.2 An energy level diagram of OH radical. The KrF excimer laser can excite transitions in the A - X(3,0) band. The fluorescence from A - X(3,2) band was detected. OH radicals in the excited upper state A(3) predissociate as well as quench.

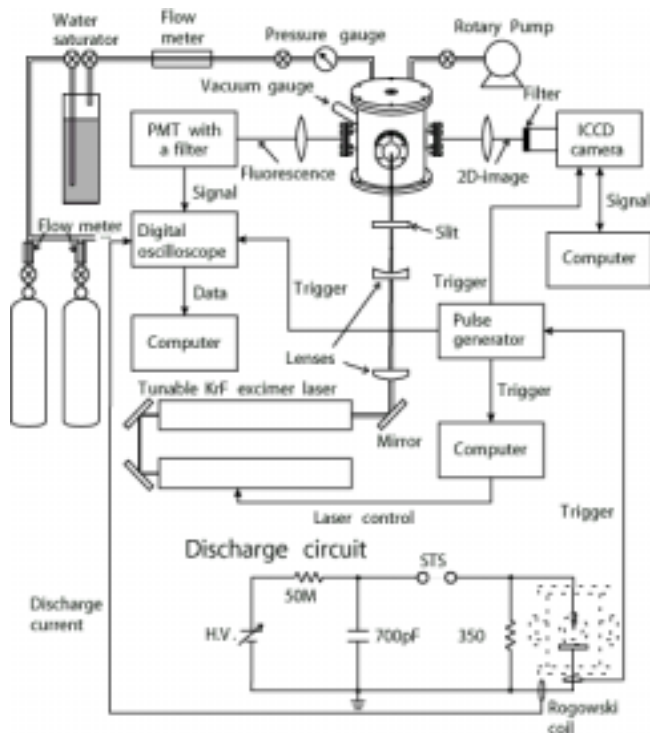


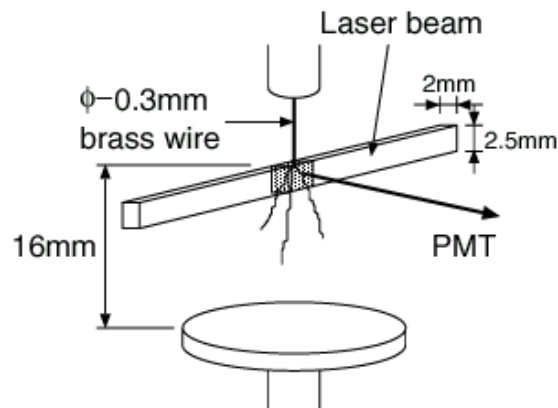
Fig.3 The schematic diagram of the experimental setup including discharge power supply. PMT: photo-multiplier, STS:self-trigger spark gap switch [22]

As already shown in Eqs.(3),(4), the quenching rate Q_2 influences on the intensity of I_{LIF} . Q_2 is affected by many factors such as temperature, pressure, and gas composition so that the determination of Q_2 is very complex. At lower pressure, Q_2 is so small that Z_2 in Eq.(4) can be approximated to A_2 . In that case, I_{LIF} is not influenced by Q_2 . On the other hand, Q_2 becomes large at atmospheric pressure and Z_2 is nearly equal to Q_2 . The typical ratio of Q_2/A_2 is about 1000 for OH radicals [18]. As a result, I_{LIF} is inversely proportional to Q_2 . The correction for Q_2 is necessary but it is not so easy.

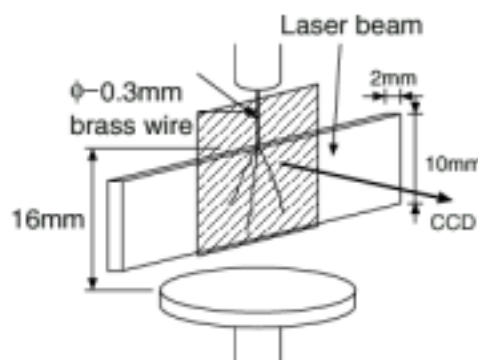
Use of a KrF laser releases that quenching problem. Figure 2 shows an energy level diagram of OH radical. Excitation and fluorescence transitions are also shown in that Fig.2. OH radicals excited to $A(3)$ state by a KrF laser predissociate in addition to quenching. The predissociation rate P_2 is determined naturally and not affected by any factors. Because P_2 is larger than Q_2 at atmospheric pressure (typically $P_2/Q_2 \sim 10$), Z_2 is approximated to P_2 . As a result, I_{LIF} is independent of Q_2 . This technique is called LIPF (laser-induced predissociative fluorescence). LIPF can reduce the quenching effect although the laser power must be high.

3.3 Experimental setup

The experimental setup used by the authors [21] is shown in Fig.3. A tunable KrF laser irradiates discharge plasma area and excites OH radicals. The fluorescence of OH radicals is detected with a PMT (photo-multiplier tube) or an gated ICCD camera through a optical bandpath filter which transmits emission from the $A - X(3,2)$ band at around 297 nm. A pulsed corona discharge is generated between needle-plate electrodes with a gap length of 16 mm. The typical applied voltage is 35 kV and the pulse width of current is about 50 ns. A signal pulse generator is triggered by a discharge current and sends trigger pulses to the laser and fluorescence detecting systems. That signal pulse generator has a time delay function, which enables to observe OH radicals in the post-discharge region. The system can measure a time evolution of OH density after the pulse discharge. Fig. 4 shows electrodes, a laser beam, and an observation volume. A 2×2.5 mm laser beam irradiates near the tip of the needle electrode. In this case, OH radicals in the hatched gray area are detected.

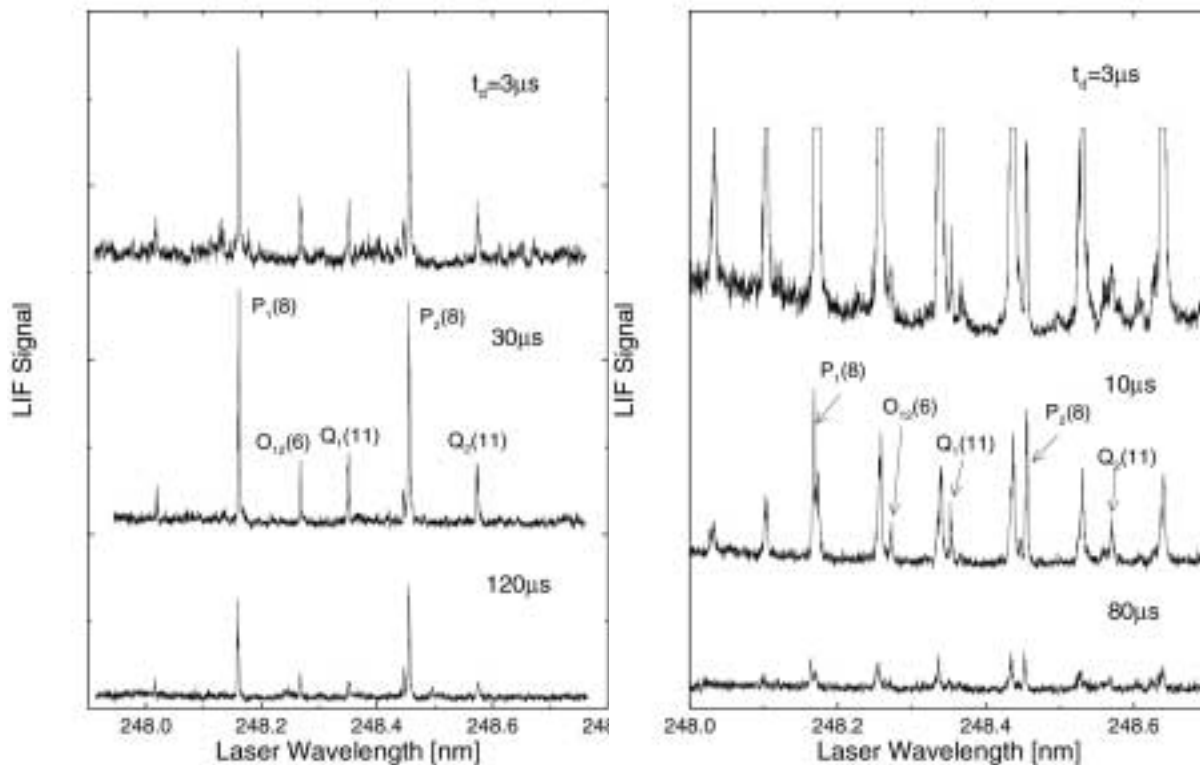


(a) total LIF signal measurement at one point where photomultiplier (PMT) is used as a detector.



(b) two-dimensional measurement beam pattern where a gated ICCD camera is used as a imaging detector.

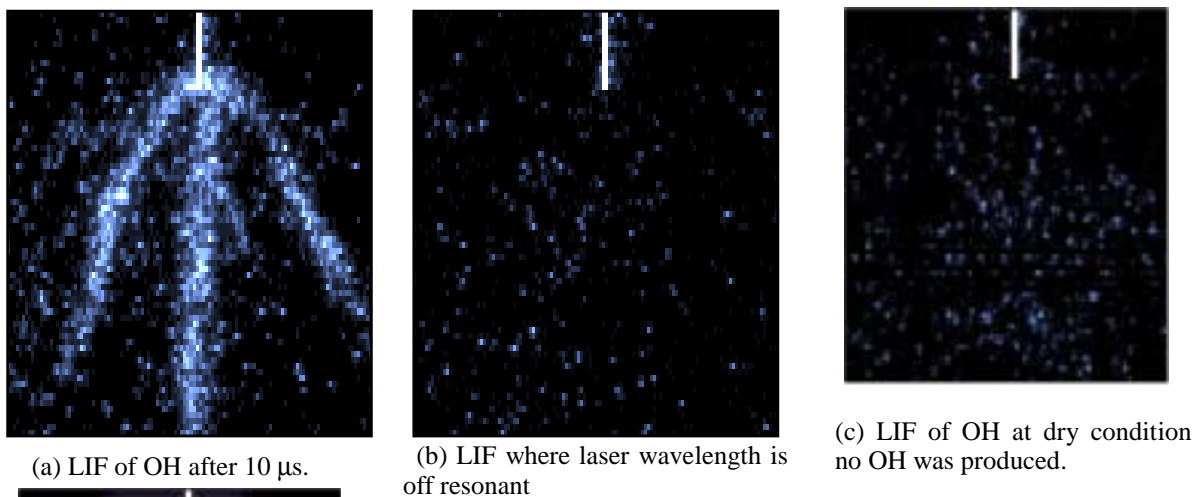
Fig. 4 The irradiation laser beam pattern and needle-plate discharge electrodes.



a) LIF spectra of the plasma in the 3 % H₂O in N₂ where each spectrum was observed at 3, 30, 120 spectrumμs after the pulse discharge.

(b) LIF spectra of the plasma in the 3% H₂O in 10 % O₂ and 87% N₂ where each was observed at 3, 10, 80 s after the discharge.

Fig. 5 LIF spectra versus exciting laser frequency.



(a) LIF of OH after 10 μs.

(b) LIF where laser wavelength is off resonant

(c) LIF of OH at dry condition no OH was produced.

(d) N₂ discharge emission pattern.

Fig. 6 Two-dimensional OH LIF profile and optical emission pattern excited by pulsed positive corona between needle-plate electrodes. A white line shows a needle electrode. (a) ~ (c) are LIF signal pattern observed at 10 μs after the discharge and (d) is real discharge emission optical image which is much strong light at other wavelength (recorded without bandpass filter).

That LIF can observe the two-dimensional density distribution by using 2D-LIF technique, which is shown in Fig.4(b). A gated ICCD camera can record the image of the OH fluorescence profile. The OH fluorescence proportional to the OH density that enables to measure OH radical density profile by one shot laser irradiation.

3.4 LIF excitation spectrum

OH fluorescence is detected when the laser wavelength is adjusted to resonant frequency of the OH absorption lines. If the laser wavelength is continuously shifted, LIF signal appears at specific wavelengths. The spectrum can be used to check whether there are some interference signals except from OH radicals. Figure 5 (a) shows LIF excited spectra in humid nitrogen gas plasma.

Fig. 5 (b) shows the LIF spectra in humid $O_2(10\%)N_2$ mixture gas where all experiments were held at atmospheric pressure otherwise the pressure must be written. There are many intensive lines except OH signals. They are LIF signals of excited O_2 molecules O_2^* [18]. At 3 s after the discharge, OH lines of $P_1(8)$, $O_{12}(6)$, $Q_1(11)$, and $Q_2(11)$ are dominated by O_2^* signals. That spectrum suggested that OH radical measurement is impossible through those lines. Although $P_2(8)$ line is slightly overlapped with O_2^* , $P_2(8)$ transition is possible to use as OH diagnosis. In all other experiments, the laser wavelength is set to $P_2(8)$.

3.5 2D-LIF observation

Two-dimensional distribution of OH radicals in the discharge plasma can be monitored by 2D-LIF. One example is shown in Fig.6(a). Comparing OH profile in Fig.(a) with streamer image in Fig.(d) indicates that OH radicals are generated in the streamers region.

Unfortunately, both figures are recorded at different discharges and exact equality cannot be determined. To enhance that equality, two other pictures are also shown. Fig. 6 (b) shows a similar picture recorded the same ICCD camera where the laser wavelength is off resonant with $OH:P_2(8)$ transition and Fig. (c) shows other picture recorded in dry environment (less OH). If some background or stray light exists in Fig.(a), they should also appear in Fig.(b). If LIF signals from other species (not OH) are recorded in Fig.(a), they also appear in Fig.(c). OH radicals disappear in dry environment because OH radicals are produced by the dissociation of H_2O molecules. Figs. (a) and (c) suggest no signals, indicating that all signals in Fig.(a) are surely due to OH radicals.

3.6 The effect of discharge conditions on generation of OH radicals

The parameter optimization such as discharge voltage, discharge current, discharge mode and environmental conditions (gas compositions) for OH production is essential for toxic gas removal in the contaminated flue gas or air because large number of OH radicals may leads to high decomposition rate of that toxic gas. In order to know those tendencies, some parameters which assumed to influence on OH radical generation are tested

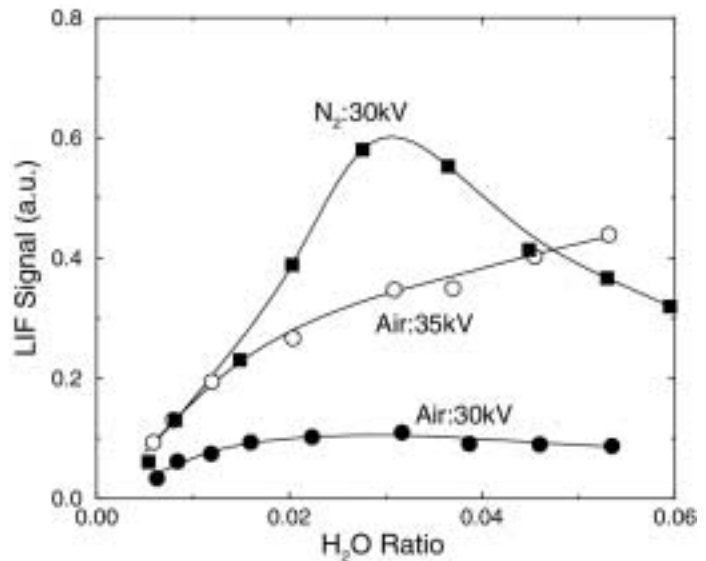


Fig. 7 OH density (LIF signal of OH) versus water concentration in the pulsed corona in nitrogen or air.

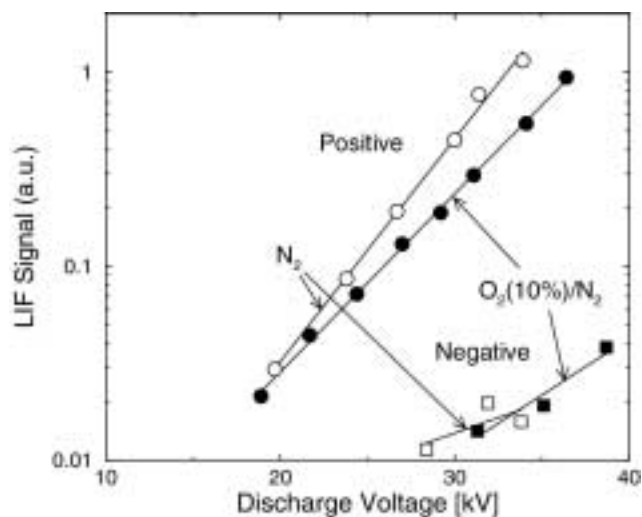


Fig. 8 OH density (LIF signal) in wet pure nitrogen or wet nitrogen with 10 % oxygen versus applied voltage of pulse.

experimentally. Fig. 7 shows the relation between OH radicals and H₂O concentration at 3 conditions. As OH radicals are formed by the dissociation of H₂O molecules, OH density increases with H₂O concentration when water concentration is low of a few percent. However, OH production saturates at some H₂O concentration or OH density decreases with increasing H₂O concentration when no oxygen was mixed. As the sensitivity of LIF is not so good, low voltage discharge mode is not yet tested. Recent results suggest that the optimum H₂O concentration should exist for OH generation in any case.

Fig. 8 shows the LIF signal intensity dependence on the applied voltage at the same discharge conditions. It shows that positive discharge yields larger amount of OH radicals than that by the negative discharge. OH density increases exponentially with applied voltage. The incident discharge energy also increases exponentially with voltage, so that the generation of OH radicals is apparently proportional to the discharge energy. By the way, Fig. 8 suggests that the large voltage yields much OH radicals but energetic efficiency of the OH radical generation is not sure.

3.7 Monitoring chemical reaction

As already shown in some date, LIF diagnosis can supply much information that is necessary to analyze the chemical reaction in the plasma. Moreover, decay signals of OH radicals with different conditions suggest existing of some chemical reactions related with OH radicals. Fig. 9 shows the time evolution of OH radicals where the nitrogen gas contains different concentrations of NO, indicating the OH-NO reactions. Addition of NO accelerates OH decay rate.

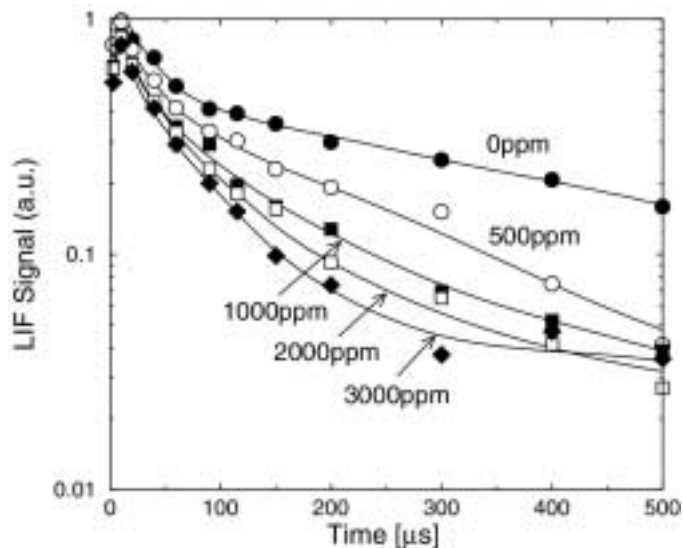


Fig.9 Time evolution of LIF signals (OH density) for various concentration of NO in humid nitrogen (arc like plasma).

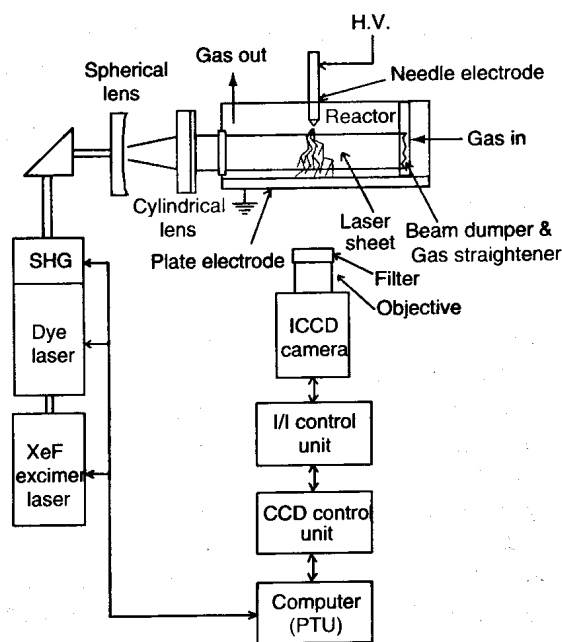


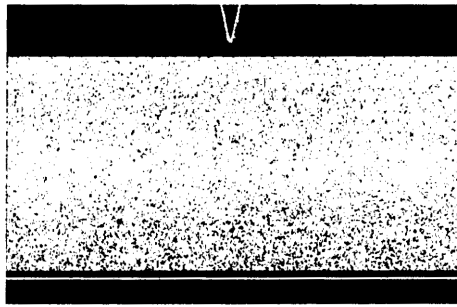
Fig. 10 The schematic diagram of NO LIF experimental setup for DC corona.

4 Laser Induced Fluorescence (LIF) for NO molecules

In Japan, several groups have been engaged in NO radical measurement by LIF with a dye laser system. Two works will be introduced.

4.1 DC corona discharge: decomposition and generation of NO[23]

Oita University group introduced NO observation LIF system which was developed for combustion flame analysis with a tunable excimer laser system. Their experimental setup is shown in Fig. 10. In that system, frequency doubled dye laser (driven by a tunable excimer laser) excites NO molecules in the vibrationally ground state via A – X(0,0) band at 226 nm. That frequency NO-LIF spectroscopy is widely used at



(a) NO LIF pattern before discharge



(b) NO LIF pattern during DC discharge at 21 kV

Fig.11 NO LIF pattern (white) before and during DC pulsive corona discharge..

atmospheric pressure combustion flame plasma analysis. As shown in the Figure, a reactor contains one set of needle-plate electrodes which can decompose NO molecules. When DC high voltage is applied to a needle electrode, a large number of small corona pulses occur between electrodes that frequency is several kHz.

Figure 11 presents 2D-LIF photos of NO molecules without and with discharge. That tested gas contains 200 ppm of NO in nitrogen. Without discharge as shown in Fig.11 (a), NO molecules should distribute uniformly in the reactor and NO-LIF signal should appear just in the laser sheet-like beam where the signal intensity should be proportional with the laser beam intensity if optical lens system is uniform. The black area in Fig. 11(a) does not mean that NO density is 0 ppm. It means that the laser beam does not irradiate the black region.

Fig. 11(b) shows NO LIF signal during DC pulse corona suggesting the perfect removal of NO in the whole region of the reactor and generation of NO molecules by the discharge. In upper stream region of the reactor, NO molecules disappear after a few minutes of DC corona although the gas flows from left to right. One may expect that NO molecules disappear just in the discharge region where plenty of fast electrons and reactive radicals exist. But the figure shows different tendency. The reason of that phenomenon is not yet clear but will be discussed at the meeting by one of research member. Moreover, a small amount of NO molecules yield in the discharge region. Those experimental results will supply a great deal of information of NO decomposition channels.

4.2 NO removal by the pulse discharge

Other ETL group is also engaged in NO LIF measurement during long time[24]. They reported the NO decay with time after one single pulse (streamer) corona as shown in Fig. 12. Just after the discharge, NO decomposition in the streamer region can be identified. At a few ms after the single submicrosecond pulse discharge, NO decomposition becomes maximum when NO concentration is low, which tendency was also observed by our experiment where we use different kind of pulse discharge.

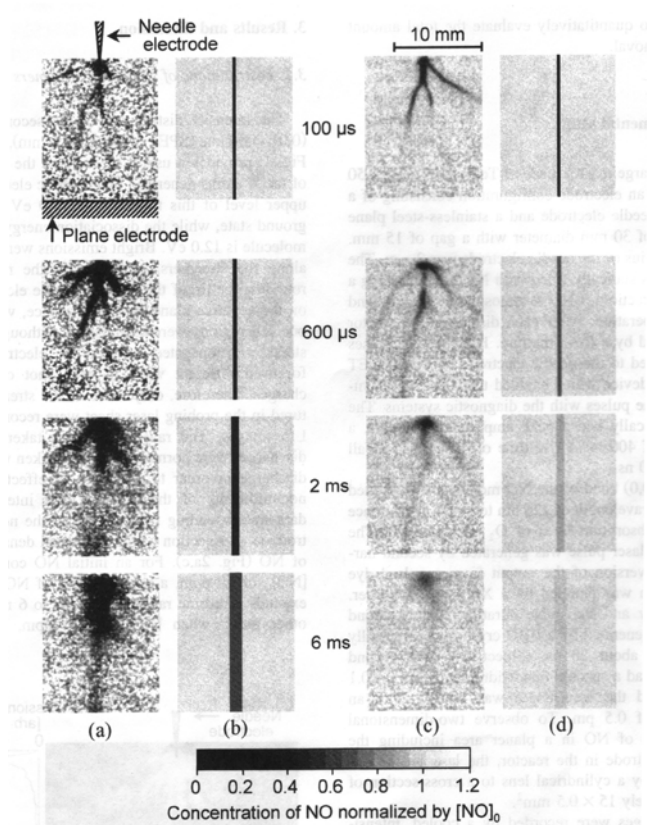


Fig.12 Distribution of NO (a,c) measured by LIF imaging spectroscopy after 23kV pulse discharge where initial NO concentration $[NO]_0$ are 30 ppm for (a) and 1,000 ppm for (c) and discharge energy is about 9 mJ. (b,d) show NO concentration along single streamer calculated with a simple model where $[NO]_0$ are 30 ppm for (b) and 1,000 ppm for (d).

5 Conclusions

Better understanding of plasma chemical reaction mechanisms in the non-thermal plasma and even in the thermal plasma at atmospheric pressure, various radical behavior in the plasma region must be investigated. That is very important to study and to develop to the practical application of the (non-)thermal plasma decomposition system for toxic gaseous components in the flue gas or in the air where the plasma chemical process must be dominant. Especially, behavior of reactive radicals such as N, O, and OH, and toxic gases such as NO_x and various VOCs must be investigated in details. Recently, non-thermal plasma processing is assumed to be effective in decomposing other PFC which is mainly used in semiconductor process and harmful as large green house effect. LIF technology is found to be a very powerful and practically useful method to identify those radicals/molecules in (non-)thermal plasma with time and two dimensional space resolutions. Other advantage of that method is that is non-intrusive and *in site* technique although experimental setup is very expensive. LIF and other spectroscopic diagnosis system are promising tools for investigation of non-thermal plasma at atmospheric pressure. The diagnosis of atmospheric pressure plasma by that LIF is not yet advanced because of expense and low sensitivity but will be improved and the most powerful research methods for the high pressure plasma..

6 Acknowledgements

The authors appreciate to Prof. Ohkubo at Oita University, Prof. Mizuno at Toyohashi University of Technology, Dr. Fujiwara at ETL, Prof. Tezaki and Dr. Shimizu for their advices. The authors also thank Prof. Muraoka and Prof. Doebele to give us a chance to present this paper. NO LIF works by Mr. Obata and Mr. Mashiko by us are also appreciated. That work is supported in part by a Grand-in-Aid for Scientific Research from the Ministry of Education of Japan.

7 References

- [1] J.S.Clements, A.Mizuno, W.C.Finney and R.H.David, IEEE Trans.Ind.Appl. **25**, (1989)pp.62-69
- [2] K.Ohtsuka, Yukitake, Shimoda, Proc.Inst.Electrost.Jp, **9**, (1985) p.346 (in Japanese)
- [3] S.Masuda and H.Nakao, Conf.Rec.IEEE/IAS Ann.Meeting, (1986), pp.1173-1182
- [4] T.Yamamoto et al, IEEE Trans.Ind.Appl., **28**, (1992), pp.528-534
- [5] T.Oda, T.Takahashi, H.Nakano and S.Masuda, IEEE Trans.Ind.Appl., **29**, (1993), pp.787-792
- [6] O.Tokunaga and N.Suzuki, Radiat.Phys.Chem., **24**, (1984), pp.145-165
- [7] Hakota et al, J.Adv.Oxid.Technol., **3**, (1998), p.79
- [8] T.Wakabayashi et al., Proc.9th Symp.Plasma Chem., (1989), pp.L111-L116
- [9] T.Oda, T.Takahashi and K.Yamaji, Cof.Rec.IEEE/IAS, (2000), file22_04
- [10] J. J. Lowke and R. Morrow, IEEE Trans. Plasma Sci., **23**, pp.661-671 (1995)
- [11] B. M. Penetrante, J. N. Bardsley and M. C. Hsiao, JJAP, **36**, (1997), pp.5007-5017
- [12] F.Tochikubo and T.H.Teich, JJAP, 39, (2000), pp.1343-1350
- [13] G.S.Selwyn, JAP., **60**, (1986), pp.2771-2774
- [14] R.M.Roth, K.G.Spears and G.Wang, Appl.Phys.Lett., **45**, (1984), pp.28-30
- [15] A. Kono, N. Koike, K. Okuda, and T. Goto, Jpn. J. Appl. Phys., **32**, (1993) pp.L543-L546
- [16] J. Bittner, A. Lawitzki, U. Meier, and K. Kohse-Höinghaus, Appl. Phys. B, **52**, (1991), pp.108-116
- [17] N. Georgiev and M. Alden, Spectrochimica Acta Part B, **52**, (1997), pp.1105-1112
- [18] E. W. Rothe and P. Andresen, Appl. Opt., **36**, (1997), pp.3971-4033
- [19] A. Gulati and R. E. Warren Jr., J. Propulsion Power, **10**, (1994), pp.54-61

- [20] P. Pezé, A. Paillous, J. Siffre, and B. Dubreuil, *J. Phys. D: Appl. Phys.*, 26, (1993), pp.1622-1629
- [21] R. Ono and T. Oda, *IEEE Trans. Ind. Appl.*, 36, (2000), pp.82-86
- [22] R. Ono and T. Oda, *Proc. IEJ-ESA Joint Symp. Electrostat.*, (2000), pp.287-296
- [23] S. Kanazawa, T. Ito, Y. Shuto, T. Ohkubo, Y. Nomoto, and J. Mizeraczyk, *Proc. 2000 Ann. Meeting Inst. Electrostat. Jpn*, (2000), pp.153-154 (in Japanese)
- [24] H.Hazama, M.Fujiwara, M.Tanimoto, *Chem.Phys.Lett.*, 323, (2000), pp.542-548